



Society of Petroleum Engineers

**SPE-191780-MS**

## **Enhanced Oil Recovery in Eagle Ford: Opportunities Using Huff-n-Puff Technique in Unconventional Reservoirs**

Piyush Pankaj, Herman Mukisa, Irina Solovyeva, and Han Xue, Schlumberger

Copyright 2018, Society of Petroleum Engineers

This paper was prepared for presentation at the SPE Liquids-Rich Basins Conference-North America held in Midland, TX, USA, 05-06 September 2018.

This paper was selected for presentation by an SPE program committee following review of information contained in an abstract submitted by the author(s). Contents of the paper have not been reviewed by the Society of Petroleum Engineers and are subject to correction by the author(s). The material does not necessarily reflect any position of the Society of Petroleum Engineers, its officers, or members. Electronic reproduction, distribution, or storage of any part of this paper without the written consent of the Society of Petroleum Engineers is prohibited. Permission to reproduce in print is restricted to an abstract of not more than 300 words; illustrations may not be copied. The abstract must contain conspicuous acknowledgment of SPE copyright.

---

### **Abstract**

Although hydraulic fracturing in liquid-rich unconventional reservoirs (LUR) has become a norm, the recovery factor continues to be low. Use of enhanced oil recovery (EOR) techniques in LUR has recently become more popular to improve the recovery. The objective of this study is to numerically investigate the advantages and disadvantages of the application of the CO<sub>2</sub> huff-n-puff technique in LUR formations having complex fracture networks.

The study explores the fluid flow mechanisms for oil recovery in a naturally fractured reservoir. A calibrated 3D mechanical earth model with geomechanical and petrophysical properties from the Eagle Ford was used for the study. A complex hydraulic fracture model was used to simulate the hydraulic fracture, proppant, and fluid distribution around the wellbore. Numerical reservoir simulation on perpendicular bisection (PEBI) grids was used to capture the permeability, porosity, and conductivity distribution due to the proppants in the hydraulic fractures. The CO<sub>2</sub> huff-n-puff technique using numerical reservoir simulation was used to determine the well performance and recovery factor arising from reservoir fluid viscosity reduction and gas expansion. The effect of fluid thermodynamics to recovery systems in the low-permeability reservoir medium was fully captured in this approach. An equation of state prepared for simulating the CO<sub>2</sub> impact on the oil was prepared with correlating the collected downhole oil sample.

The numerical reservoir simulation study coupled with the complex fracture simulation model presents insights into a new means to improve the recovery factor (RF) in LUR through the injection of CO<sub>2</sub>. Such EOR method would be critical to increase the long-term economic benefits. The study demonstrates that that infill well requirements can be mitigated if the EOR method of huff-n-puff is utilized in cyclic modes over various time periods of production. Up to 9% extra RF was observed when the CO<sub>2</sub> huff-n-puff technique was used as compared to production dependent only on hydraulic fracture stimulation. Parametric sensitivity on job sizes and start timing of EOR in a producing well was used to evaluate the RF. However, the hydraulic fracture geometry and the created footprint along with the time of injection have a larger effect in improving the EOR effectiveness.

The methodology demonstrates the simulation of EOR methods in unconventional reservoirs for economic assessment. The workflow demonstrates modeling CO<sub>2</sub> flooding as an EOR technique on the full

wellbore level with complex hydraulic fracture geometry. The approach can be applied to unconventional formations in other basins to improve the recovery factor.

## Introduction

The use of multiple-stage hydraulic fracturing on a horizontal well allows maximized contact between the well and the reservoir matrix by means of connecting with naturally occurring and microfractures. Enhanced surface area in contact with the wellbore greatly increases the chances for economic oil production rates in the ultralow-permeability shale formations. However, most unconventional liquid shale wells suffer from rapid production decline, and the production rate stagnates at a low rate. One such unconventional formation is the Eagle Ford formation, which is recognized as one of many world-class source rocks and has been producing approximately 2 billion barrels of oil since the horizontal discovery well STS #1 in 2008. The estimates of oil recovery during primary production range from 5 to 10% of original oil in place, leaving a huge amount of potential underground. As such, the prize is so large, it becomes essential to continue to evaluate techniques of improved oil recovery in unconventional reservoirs beyond multistage hydraulic fracturing. The technology for CO<sub>2</sub> EOR in unconventional oil plays is still in the early stages of development.

## Huff-n-Puff Pilot

Much of the work around improved oil recovery (IOR) and enhanced oil recovery (EOR) for unconventional reservoirs has been focused on gas injection methods. In addition to the type of fluid injected, an important characteristic of an injection process is the method of delivery. Although most conventional situations use a continuous injection process with dedicated offset injection and producing wells, some fields use a cyclic injection process in which a single well serves as both the injector and the producer. This is also sometimes called a huff-n-puff process. The technique typically includes three steps: first is the injection phase; then the well is shut in for the soak phase; and, finally, the well is turned back on for the production phase (Fig. 1). This has had the most success in steam injection, but it has also been used to a limited extent during CO<sub>2</sub> injection in conventional reservoirs.

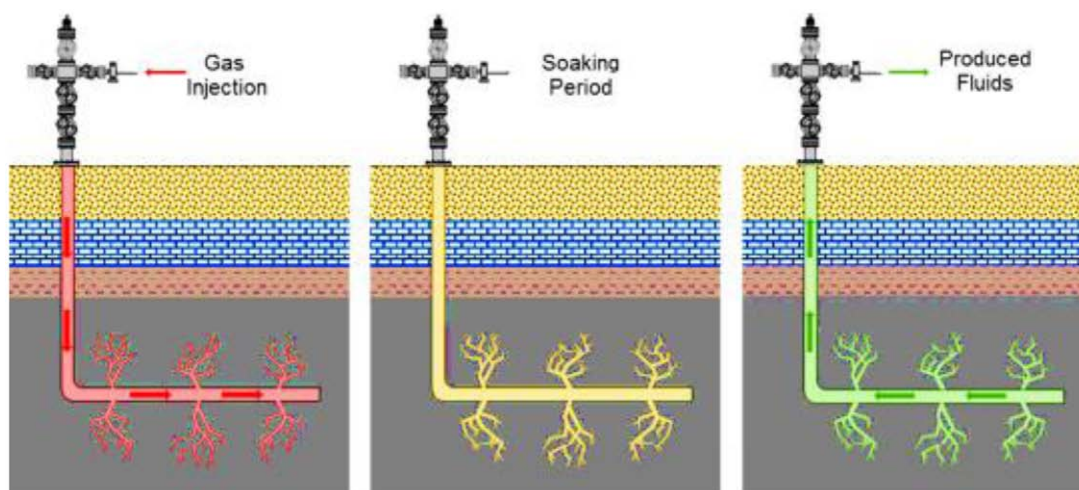


Figure 1—Huff-n-puff technique using CO<sub>2</sub> injection for enhanced oil recovery (EOR).

There have been many field trials (also known as pilot projects) in unconventional reservoirs, particularly in the Bakken and Eagle Ford. Over most of the last decade, application of the EOR techniques for unconventional reservoirs has been limited to a limited number of operators. However, reports of success with huff-n-puff gas injection in the Eagle Ford has prompted a rapidly growing interest over the last couple

years, especially with the [Thomas et al. \(2016\)](#) report that wells could produce 30% to 70% more oil after huff-n-puff gas injection was deployed. A study by [Hoffman \(2018\)](#) concluded that the huff-n-puff natural gas injection pilots have shown that this process will recover additional oil in the oil window of the Eagle Ford. This is confirmed with multiple other pilot tests conducted by various operators spread around in the area. Production economics during these pilots appear to be marginally successful for many operators. However, as more pilots and fieldwide development occurs, improved efficiencies and better reservoir understanding should realize improved economics as well. In shale gas or oil reservoirs, the presence of fissures or induced hydraulic fractures provides highly conductive paths for injected gas during a huff-n-puff operation to diffuse or penetrate the nano-Darcy permeability matrix. The Eagle Ford pilots have been almost exclusively hydrocarbon gas injected (presumably due to the availability of the injectant) with the huff-n-puff method.

Overall, the results are very encouraging. There are some similarities among the different projects; for instance, they all use huff-n-puff with natural gas and are carried out in the black oil region of the Eagle Ford. The pilots are spread over 100 miles of the Eagle Ford conducted by different operators where the injected gas composition was different from each other. Although it is difficult to estimate the amount of incremental recovery due to limitations with the public data, all pilots demonstrated an increase in oil production rates ([Hoffman 2018](#)).

### **Laboratory Findings for Modified CO<sub>2</sub> Core flooding for Fractured Shale**

[Gamadi et al. \(2014\)](#) conducted experimental work on shale cores from the Mancos and Eagle Ford formations to investigate potential of CO<sub>2</sub> injection in these reservoirs. Their laboratory results indicated that cyclic CO<sub>2</sub> injection could improve oil recovery from shale oil cores from 33% to 85% depending on the shale core type and other operating parameters. [Tovar et al. \(2014\)](#) presented a thorough evaluation of CO<sub>2</sub> injection in organic-rich shale. They started by demonstrating that direct gas injection through organic-rich shale matrix is not possible in a reasonable time frame. That triggered the construction of equipment and the development of novel injection technique that resembled the injection through hydraulic fractures. They estimated the recovery factor was between 18 and 55% of the initial crude oil volume in the cores. Recovery factor increased with increasing the pressure and soak time. Crude oil recovery is driven by vaporization of the intermediate components of the oil into CO<sub>2</sub>, and their subsequent condensation after the gas is produced and flashed at room pressure and temperature. This demonstrated that it is possible to use CO<sub>2</sub> to extract the naturally occurring oil in core plugs with extremely low permeability, where gas cannot be injected directly. Also, by coupling the core flooding equipment developed in house to a CT (computed tomography) scanner, they demonstrated that this technology was able to track the changes in density resulting from the mass exchange between CO<sub>2</sub> and crude oil. An increase in CT number is an indication that CO<sub>2</sub> can penetrate the preserved sidewall core over time causing an overall increase in density. A huff-n-puff like exploitation scheme was implemented in the experiment. When the production stream was open, the CO<sub>2</sub> and vaporized hydrocarbon components could move out of the core, reducing the density and CT number. During the soaking process, CO<sub>2</sub> dissolved into the oil, and the lighter hydrocarbon components were vaporized into the CO<sub>2</sub>, as suggested by the appearance of the oil recovered and the CT images ([Tovar et al. 2014](#)). The changes in CT number as a function of time revealed the CO<sub>2</sub> penetrated the rock matrix rapidly after injection was started, indicating transport cannot be modeled solely by Darcy flow and an additional mechanism such as diffusion must be accounted for. [Tovar et al. \(2014\)](#) also presented a discussion of the results based on viscous displacement, diffusion, and the solubilization mechanism. [Alfarge et al. \(2017\)](#) concluded that there is a clear gap between laboratory work conclusions and pilot test performance, and this gap mainly happened due to the misleading prediction for the role of the CO<sub>2</sub> diffusion mechanism in field conditions by upscaling laboratory observations. The poor representation of the CO<sub>2</sub> diffusion mechanism in the Eagle

Ford happened was the result either of the kinetics of the oil recovery process in productive area being too fast or the CO<sub>2</sub> diffusion rate in field conditions being slow (Alfarge et al. 2017).

## Eagle Ford Case Study

Our goal is to create a coupled hydraulic fracture model and numerical reservoir simulation model based on representative Eagle Ford volatile oil window fluid data to evaluate the technical and economic feasibility for huff-n-puff injection of CO<sub>2</sub> into a horizontal well hydraulically fractured in multiple stages. Further, we investigate the preferable cyclic injection scheme with the fracture network complexity resulting from stimulation treatment scenarios. The general workflow for the study is represented in Fig. 2.

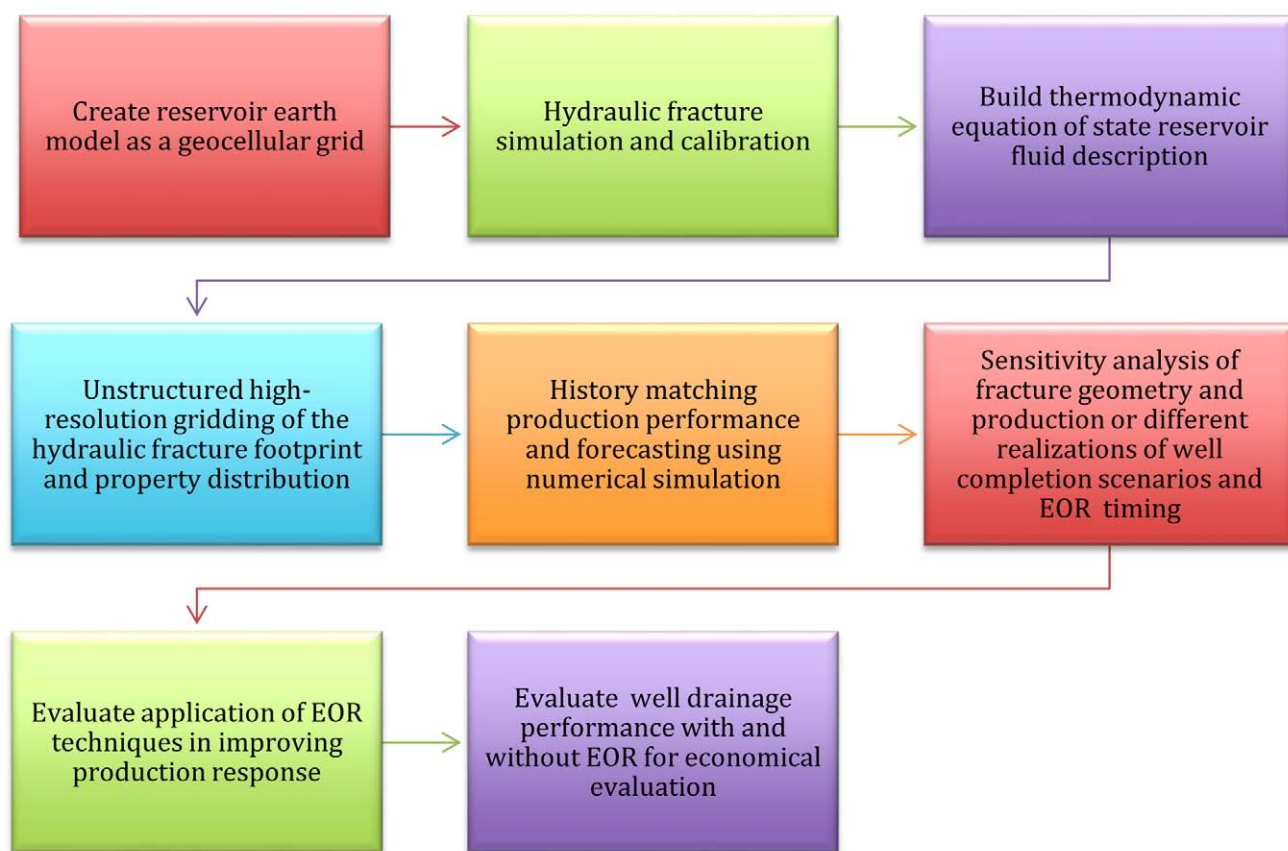


Figure 2—General workflow for the EOR application evaluation for unconventional reservoirs.

In this study, two steps of research have been integrated to investigate the parameters that control the success of the CO<sub>2</sub> huff-n-puff process at the pad scale of Eagle Ford shale oil reservoirs:

1. Historical production data were used to calibrate parent well which was hydraulically fractured.
2. Discrete simulated scenarios were created to reflect induced fracture complexity caused by different treatment design scenarios.

## Model Description

The study is carried out using a representative Eagle Ford data set that was used by Gakhar et al. (2017). A geological and geocellular model around the wellbore has been created. Petrophysical and geomechanical properties are distributed for the region around the wellbore in the depths between the Austin Chalk and Buda limestone (Fig. 3).

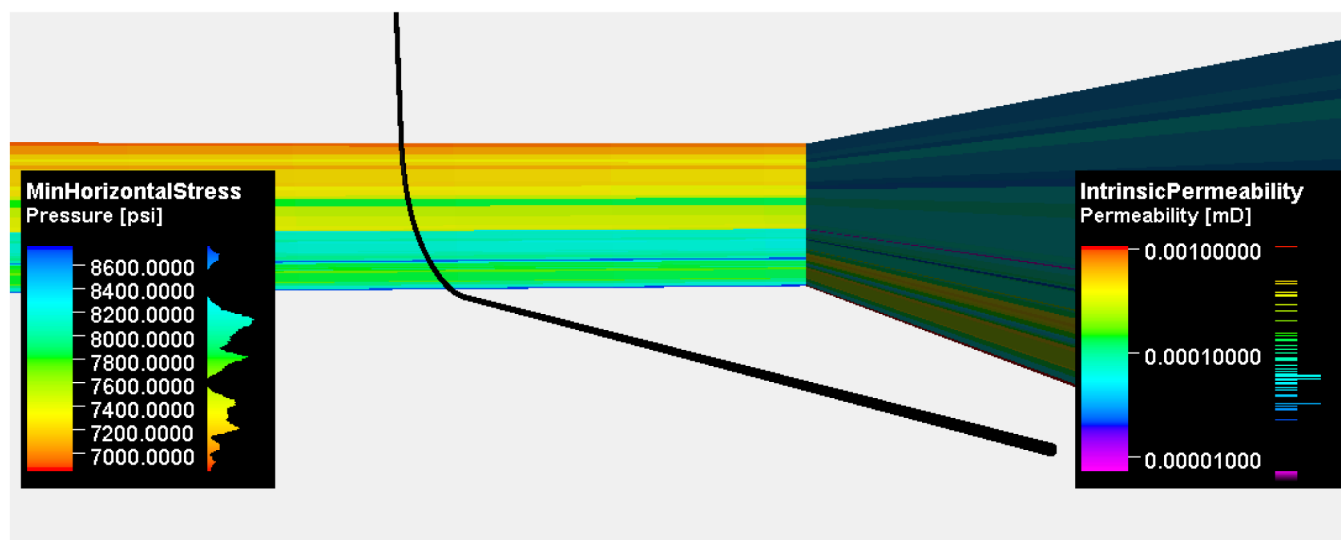


Figure 3—Wellbore landed in the lower Eagle Ford and a geomodel constructed around the wellbore with geomechanical and petrophysical properties.

We investigate the effect of fracture complexity under different treatment designs as well as the timing to start the huff-n-puff EOR application on a producing well. Our focus is the understanding of how externally controlled operational parameters can be adjusted to maximize the recovery factor under gas injection.

## Hydraulic Fracture Dynamics

The unconventional fracture model (UFM) (Weng et al. 2011) captures Mode I hydraulic fracture propagation, elastic deformation within the surrounding rock, and fluid flow in a complex fracture network. The governing equation is a fully coupled system of fluid flow in the fracture channel, fluid rheology, and mass conservation, including the potential leakoff of fracturing fluid into the rock. The interplay between hydraulic fractures and natural fractures is of particular interest. The UFM engine solves analytically the interaction of hydraulic fractures and natural fractures through a crossing criterion. If joints and fissures associated with shale play rock fabric are appropriately oriented, they will act as pre-existing planes of weakness that are likely to reactivate before reaching the stress conditions required for failure of intact rock; in this case, the hydraulic fracture may be arrested and even reactivate the natural fracture. The opening of the natural fracture takes place if the fluid pressure at the intersection exceeds the minimum compressive stress acting on the natural fracture. The reopened natural fracture can create an additional fluid conduit to the shale matrix and induced hydraulic fractures. The hydraulic fracture may also cross the natural fracture and proceed with propagation along the maximum horizontal stress direction (Weng et al. 2011). Depending on the density and properties of the natural fracture network, the hydraulic fractures may create greater complexity when the natural fractures are more densely populated. The hydraulic fracture footprint for the well in our study is shown in Fig. 4. The well was completed with 19 stages and 1,800 lbm of proppant pumped per foot of the wellbore in the simulation model.

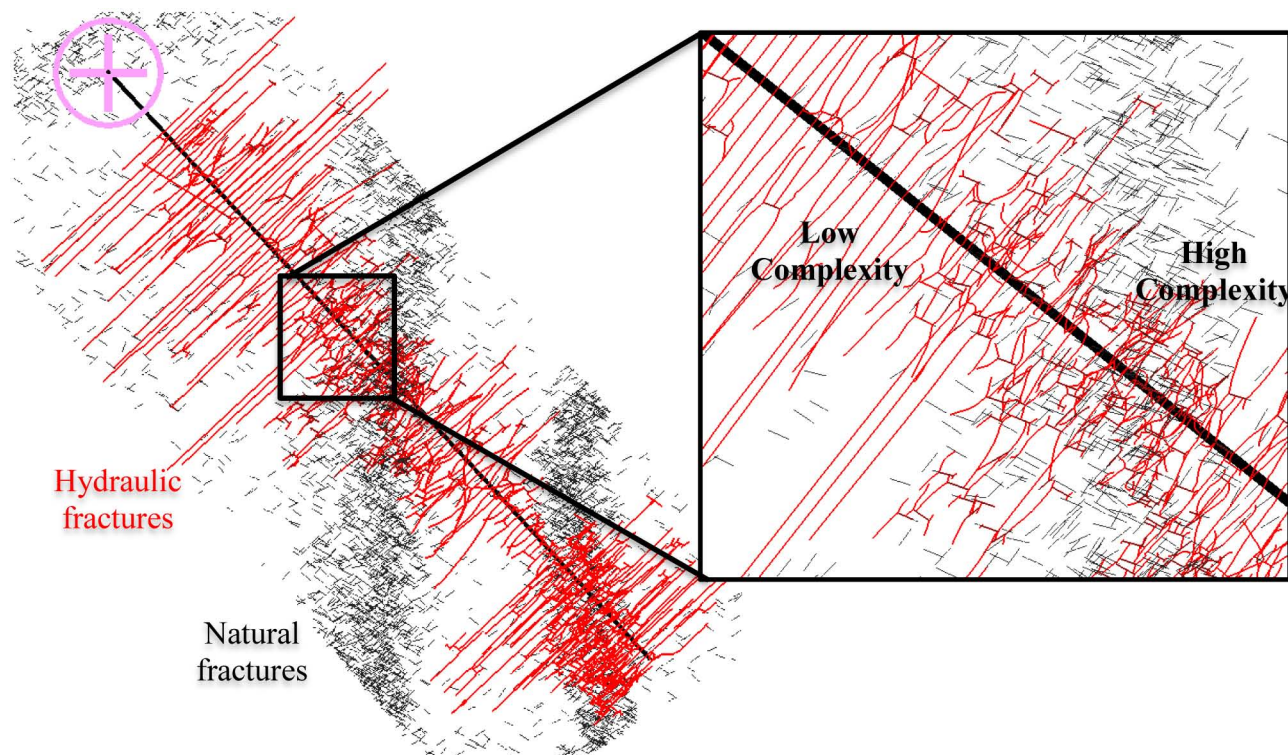


Figure 4—Hydraulic fractures and natural fracture in a top view. As the natural fracture density changes, the hydraulic fracture footprint may vary.

The induced fracture geometry, along with reactivated natural fissures, was gridded into a perpendicular bisection grid (PEBI grid). The automated gridding algorithm is described in [Cipolla et al. \(2011a,b\)](#). An advanced, fully featured numerical reservoir simulator capable of handling unstructured grid/PEBI grid patterns and solving the diffusivity equation with a controlled volume numerical scheme was used for solving fluid flow in a porous medium through an induced fracture network.

[Fig. 5](#) shows the configuration of well and the hydraulic fractures in the well from a side view. Moreover, [Fig. 5](#) demonstrates the unstructured grid created for reservoir simulation. The unstructured PEBI grid captures the variability and complexity of the hydraulic fractures and the distribution of permeability as a granular representation because the proppants in the hydraulic fractures may have settled towards the bottom of the fractures.

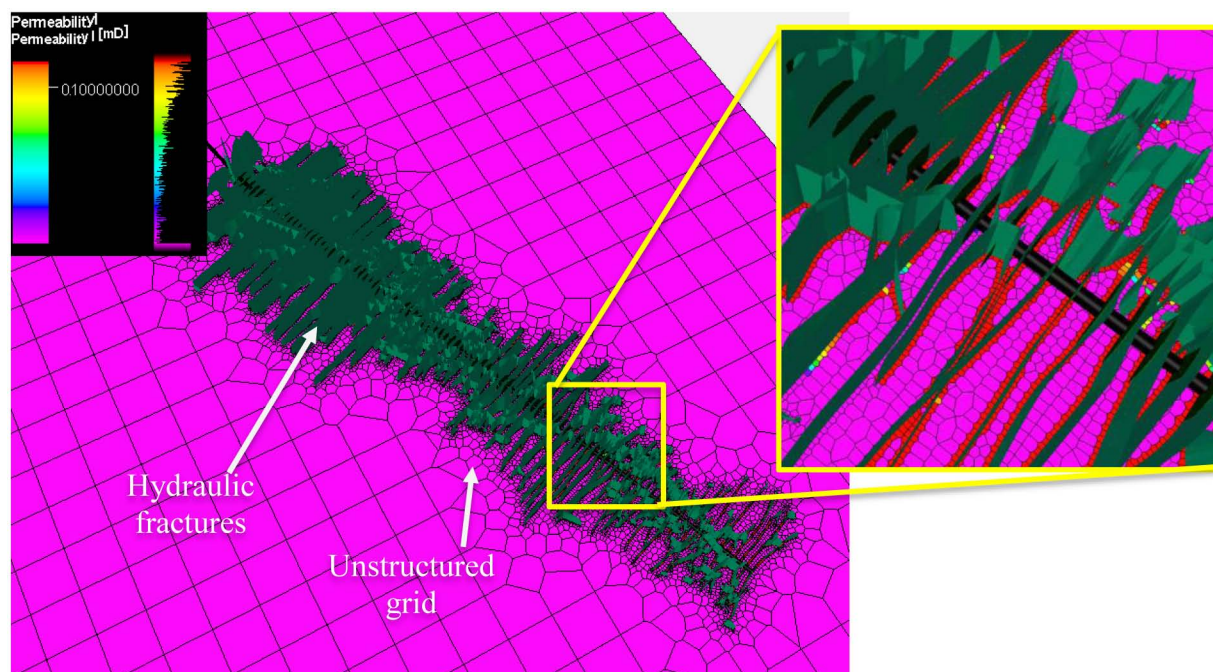


Figure 5—Hydraulic fractures and unstructured grid properties used for the reservoir simulation.

## Reservoir Fluid Model

The fluid model we chose in this study was characterized by [Orangi et al. \(2011\)](#). The fluids fall into black oil window in the Eagle Ford shale. The original composition of this oil is listed in [Table 1](#) and [Table 2](#) taken from [Orangi et al. \(2011\)](#) with the initial gas-oil ratio (GOR) of 2000 scf/day.

Table 1—Equation of state (EOS) parameters for compositional reservoir fluid model for Eagle Ford shale ([Orangi et al. 2011](#)).

**EOS Parameters for Compositional Models  
Synthetic Eagle Ford Oil**

| Comp. | Mole. Wt. | Specific Gravity | Acentric Factor | Shift   | Tc Deg R | Pc psia | Vc cft/lbM | Zcrit  | Omega A | Omega B | Composition (mole Frac) |         |         |
|-------|-----------|------------------|-----------------|---------|----------|---------|------------|--------|---------|---------|-------------------------|---------|---------|
|       |           |                  |                 |         |          |         |            |        |         |         | GOR scf/stb             |         |         |
|       |           |                  |                 |         |          |         |            |        |         |         | 500                     | 1000    | 2000    |
| C1    | 16.04     | 0.3500           | 0.0130          | -0.1540 | 343.3    | 673.1   | 1.5658     | 0.2861 | 0.4572  | 0.0778  | 0.31231                 | 0.44522 | 0.56447 |
| N2    | 28.01     | 0.8080           | 0.0400          | -0.1660 | 227.2    | 492.3   | 1.4256     | 0.2879 | 0.4572  | 0.0778  | 0.00073                 | 0.00104 | 0.00132 |
| C2    | 30.07     | 0.4800           | 0.0986          | -0.1002 | 549.8    | 708.4   | 2.3556     | 0.2828 | 0.4572  | 0.0778  | 0.04314                 | 0.05882 | 0.07288 |
| C3    | 44.10     | 0.5077           | 0.1524          | -0.0850 | 665.8    | 617.4   | 3.2294     | 0.2790 | 0.4572  | 0.0778  | 0.04148                 | 0.04506 | 0.04827 |
| CO2   | 44.01     | 0.8159           | 0.2250          | -0.0620 | 547.6    | 1071.3  | 1.5126     | 0.2758 | 0.4572  | 0.0778  | 0.01282                 | 0.01821 | 0.02306 |
| IC4   | 58.12     | 0.5631           | 0.1848          | -0.0794 | 734.6    | 529.1   | 4.2127     | 0.2827 | 0.4572  | 0.0778  | 0.01350                 | 0.01298 | 0.01251 |
| NC4   | 58.12     | 0.5844           | 0.2010          | -0.0641 | 765.4    | 550.7   | 4.1072     | 0.2754 | 0.4572  | 0.0778  | 0.03382                 | 0.02978 | 0.02615 |
| IC5   | 72.15     | 0.6248           | 0.2223          | -0.0435 | 828.7    | 483.5   | 4.9015     | 0.2665 | 0.4572  | 0.0778  | 0.01805                 | 0.01507 | 0.01240 |
| NC5   | 72.15     | 0.6312           | 0.2539          | -0.0418 | 845.6    | 489.5   | 5.0232     | 0.2710 | 0.4572  | 0.0778  | 0.02141                 | 0.01711 | 0.01325 |
| NC6   | 86.18     | 0.6641           | 0.3007          | -0.0148 | 914.2    | 439.7   | 5.9782     | 0.2679 | 0.4572  | 0.0778  | 0.04623                 | 0.03280 | 0.02076 |
| C7+   | 114.40    | 0.7563           | 0.3739          | 0.0191  | 1060.5   | 402.8   | 7.4093     | 0.2759 | 0.4572  | 0.0778  | 0.16297                 | 0.11563 | 0.07316 |
| C11+  | 166.60    | 0.8135           | 0.5260          | 0.0919  | 1223.6   | 307.7   | 10.682     | 0.2670 | 0.4572  | 0.0778  | 0.12004                 | 0.08940 | 0.05924 |
| C15+  | 230.10    | 0.8526           | 0.6979          | 0.1501  | 1368.4   | 241.4   | 14.739     | 0.2620 | 0.4572  | 0.0778  | 0.10044                 | 0.07127 | 0.04509 |
| C20+  | 409.20    | 0.9022           | 1.0456          | 0.2447  | 1614.2   | 151.1   | 26.745     | 0.2539 | 0.4572  | 0.0778  | 0.07306                 | 0.04762 | 0.02745 |

Table 2—Basic properties of the pseudo-components (Orangi et al. 2011).

**Peng-Robinson Interaction Coefficients**

|      | C1    | N2    | C2    | C3    | CO2   | IC4   | NC4   | IC5   | NC5   | NC6   | C7+   | C11+  | C15+  | C20+  |
|------|-------|-------|-------|-------|-------|-------|-------|-------|-------|-------|-------|-------|-------|-------|
| C1   | 0     | 0.036 | 0     | 0     | 0.1   | 0     | 0     | 0     | 0     | 0     | 0.025 | 0.049 | 0.068 | 0.094 |
| N2   | 0.036 | 0     | 0.05  | 0.08  | -0.02 | 0.095 | 0.09  | 0.095 | 0.1   | 0.1   | 0.151 | 0.197 | 0.235 | 0.288 |
| C2   | 0     | 0.05  | 0     | 0     | 0.13  | 0     | 0     | 0     | 0     | 0     | 0.02  | 0.039 | 0.054 | 0.075 |
| C3   | 0     | 0.08  | 0     | 0     | 0.135 | 0     | 0     | 0     | 0     | 0     | 0.015 | 0.029 | 0.041 | 0.056 |
| CO2  | 0.1   | -0.02 | 0.13  | 0.135 | 0     | 0.13  | 0.13  | 0.125 | 0.125 | 0.125 | 0.11  | 0.097 | 0.085 | 0.07  |
| IC4  | 0     | 0.095 | 0     | 0     | 0.13  | 0     | 0     | 0     | 0     | 0     | 0.01  | 0.019 | 0.027 | 0.038 |
| NC4  | 0     | 0.09  | 0     | 0     | 0.13  | 0     | 0     | 0     | 0     | 0     | 0.01  | 0.019 | 0.027 | 0.038 |
| IC5  | 0     | 0.095 | 0     | 0     | 0.125 | 0     | 0     | 0     | 0     | 0     | 0.005 | 0.01  | 0.014 | 0.019 |
| NC5  | 0     | 0.1   | 0     | 0     | 0.125 | 0     | 0     | 0     | 0     | 0     | 0.005 | 0.01  | 0.014 | 0.019 |
| NC6  | 0     | 0.1   | 0     | 0     | 0.125 | 0     | 0     | 0     | 0     | 0     | 0     | 0     | 0     | 0     |
| C7+  | 0.025 | 0.151 | 0.02  | 0.015 | 0.11  | 0.01  | 0.01  | 0.005 | 0.005 | 0     | 0     | 0     | 0     | 0     |
| C11+ | 0.049 | 0.197 | 0.039 | 0.029 | 0.097 | 0.019 | 0.019 | 0.01  | 0.01  | 0     | 0     | 0     | 0     | 0     |
| C15+ | 0.068 | 0.235 | 0.054 | 0.041 | 0.085 | 0.027 | 0.027 | 0.014 | 0.014 | 0     | 0     | 0     | 0     | 0     |
| C20+ | 0.094 | 0.288 | 0.075 | 0.056 | 0.07  | 0.038 | 0.038 | 0.019 | 0.019 | 0     | 0     | 0     | 0     | 0     |

## History Match Calibration

Numerical simulation methods have been used to history match a sample Eagle Ford well and to investigate different CO<sub>2</sub> injection scenarios. A compositional model has been used together with an unstructured grid.

Without the history matching step, the simulation might generate misleading results in EOR studies. The explicit method to model hydraulic fractures and their interaction with a natural fracture is captured in the PEBI grid. The 3D geocellular model was coupled with the calibrated fracture geometry across the entire wellbore to generate the PEBI grid, which is a unique gridding that captures the granularity for property grid orientation to facilitate flow direction from grid block to grid block during dynamic flow simulation. Matrix relative permeability is based on Corey's function, and straight line relative permeability curves were used in the fractures. During the production history match process, the simulation control was oil rate while matching GOR, water rate, and well bottomhole pressure (BHP). Initial attempts to history match indicated that the matrix permeability was high in the geomodel, and so this became one of the tuning parameters for this process. Early well performance was primarily controlled by the complex hydraulic fracture permeability and, in later time, by the matrix permeability. The maximum gas relative permeability was adjusted to control the GOR trend observed. The initial spike in water production was attributed to flowback, and no attempt was made to match this early-time data. An acceptable match was obtained with matrix average permeability of 22 nD and average hydraulic fracture permeability of 3 mD. Connate water saturation and critical water saturation are "history matched" variables that were refined during production calibration to help with the water production match.

History matching results in Fig. 6 show good agreement of simulated and measured BHP after several iterations. The GOR match can potentially be improved by considering the possibility of higher estimated matrix permeability near the fracture conduit area to create an undersaturated drainage local region. A final depletion field was obtained, reflecting the pressure state at the end of production depletion (Fig. 7). The history match obtained in this case is nonunique; however, it provides confidence for further predictions that are detailed in later sections of this paper.

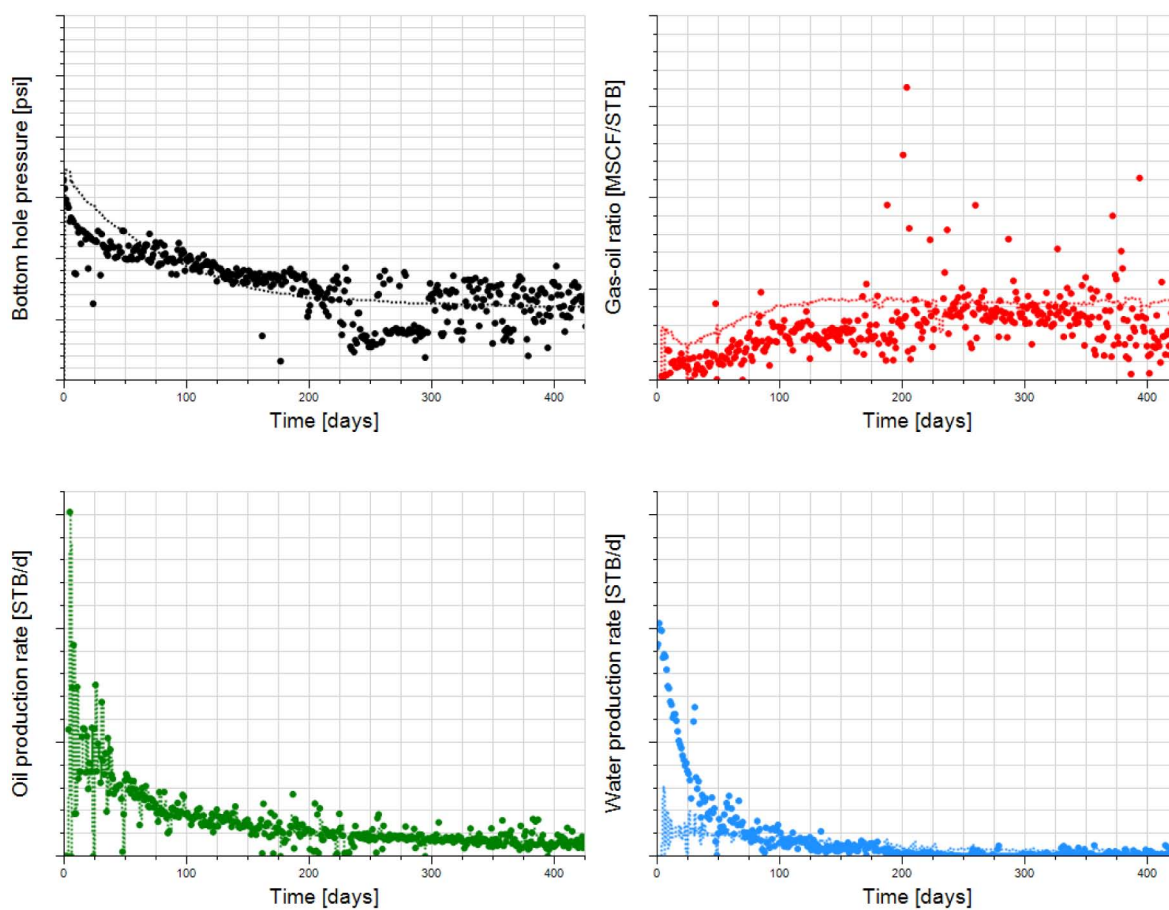


Figure 6—Production history match.

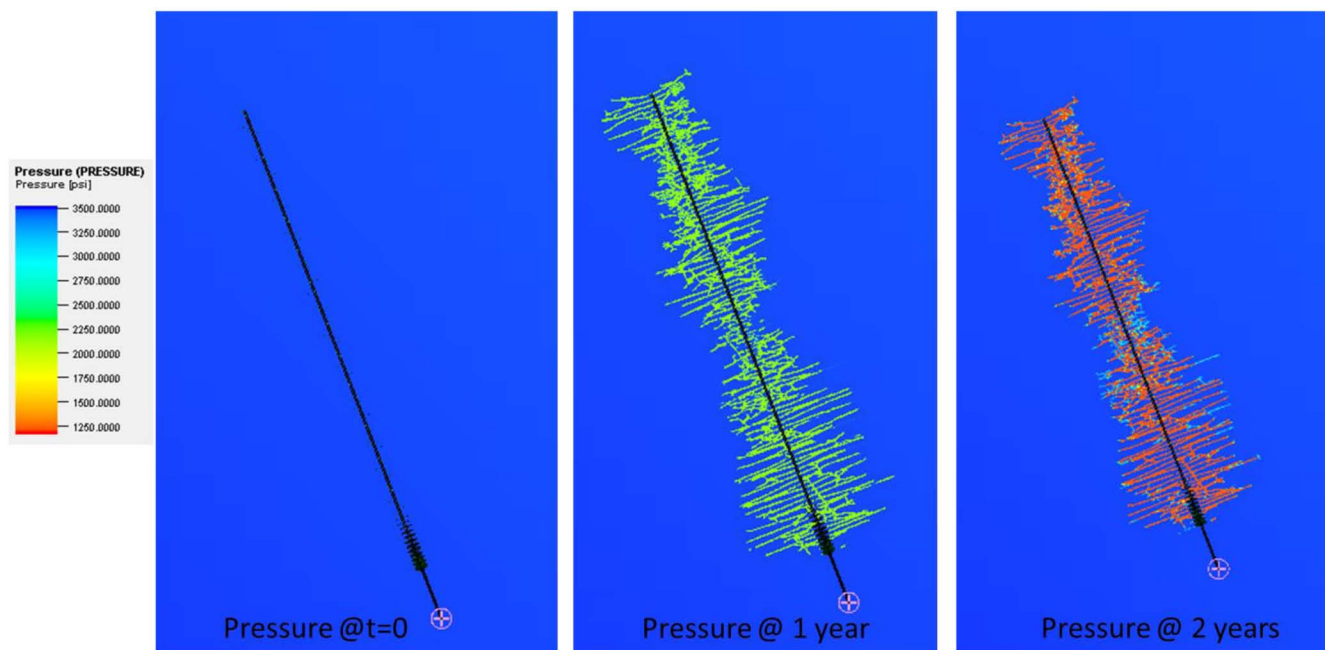


Figure 7—Pressure depletion after stimulation (no depletion) and at 12 and 24 months.

## Huff-n-Puff EOR Simulation

Two scenarios of production management are evaluated in this study: 1) A do-nothing case, with natural depletion at constant BHP following the historical production period in the parent well and 2) application of the huff-n-puff EOR technique to improve production on the parent well. Each scenario requires a simulation development strategy configuration to capture the processes correctly.

For each development strategy, three different stimulation treatment designs were tested to explore the multivariant effect of the preferable production scheme for a range of fracture complexity scenarios. The simulation was conducted to investigate the combined effect of proppant placement density and production operational control mode, such as natural depletion versus huff-n-puff. In addition, the impact of the initial start of the huff-n-puff implementation was studied.

### Natural Depletion for Eagle Ford History Matched Model

The reservoir model initially was run in natural depletion for the period of about 2 years based on available historical production data. In the numerical models, the parent well, which was hydraulically fractured, was subjected to the minimum BHP based on the last observed pressure data. In the natural depletion scenario, it was clear that the production well started with high production rate initially. Then, it showed a steep decline rate until it leveled off at a low rate. This is the typical trend to what is happening in most, if not all, the unconventional reservoirs of North America. As we investigate the pressure distribution in the reservoir model as shown in Fig. 7, we find that the main reason for the fast reduction in production rate is the pressure depletion in the area close to the production well. However, the reservoir pressure is still high in the areas that are far away from the production well. This is explained by the fact that the reservoir matrix is extremely low permeability and does not have large deliverability beyond the stimulated rock volume.

### Depletion Followed by EOR Application for Eagle Ford History Matched Model

Huff-n-puff is a multicyclic process conducted in the field with a goal to maximize economic target (i.e., cumulative produced oil in a cost-effective manner). Given the complex geologic conditions of the reservoir, induced fracture geometry, and traits of the reservoir fluid composition, there is a limit of crude oil that could be extracted by EOR process, including CO<sub>2</sub> huff-n-puff. Each cycle consists of 4 weeks of injection, 2 weeks of soaking, and 3 months of production. The beginning of the huff-n-puff was selected to be at the end of the historical period (2 years of production). The natural depletion of the parent wellbore was approximated by producing it without changing operating conditions. The comparison of results is shown in Fig. 8. A 3% increase of in cumulative oil was observed comparing natural depletion case over the time frame of 2 years. Although more cycles yield additional incremental recovery, their impact on incremental production is progressively diminished.

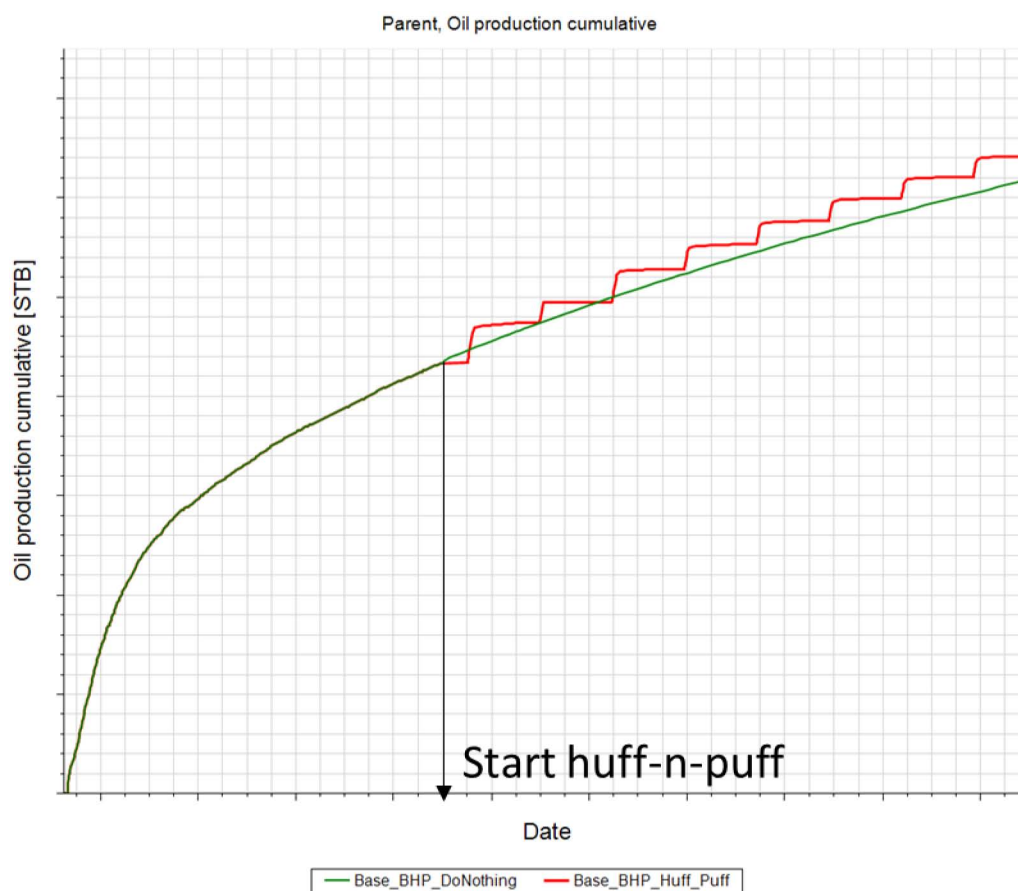


Figure 8—Cumulative oil production comparison under natural depletion vs. huff-n-puff.

## Sensitivity Studies

The next sensitivity study was carried related to effect of different treatment sizes under the same production management strategy (Fig. 9).

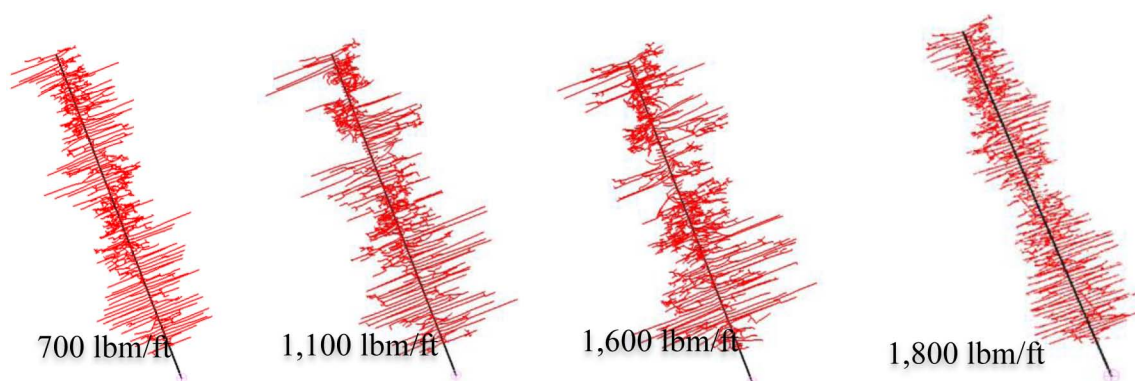


Figure 9—Fracture geometry in plan view for different treatment size.

It was observed that higher treatment sizes lead to greater network complexity, which favors gas contacting a larger fracture surface area, which, in turn, leads to higher efficiency in terms of incremental production (Fig. 10 and Table 3). The hydraulic fracture network complexity favors the natural depletion as well due to the additional reservoir surface area contact created.

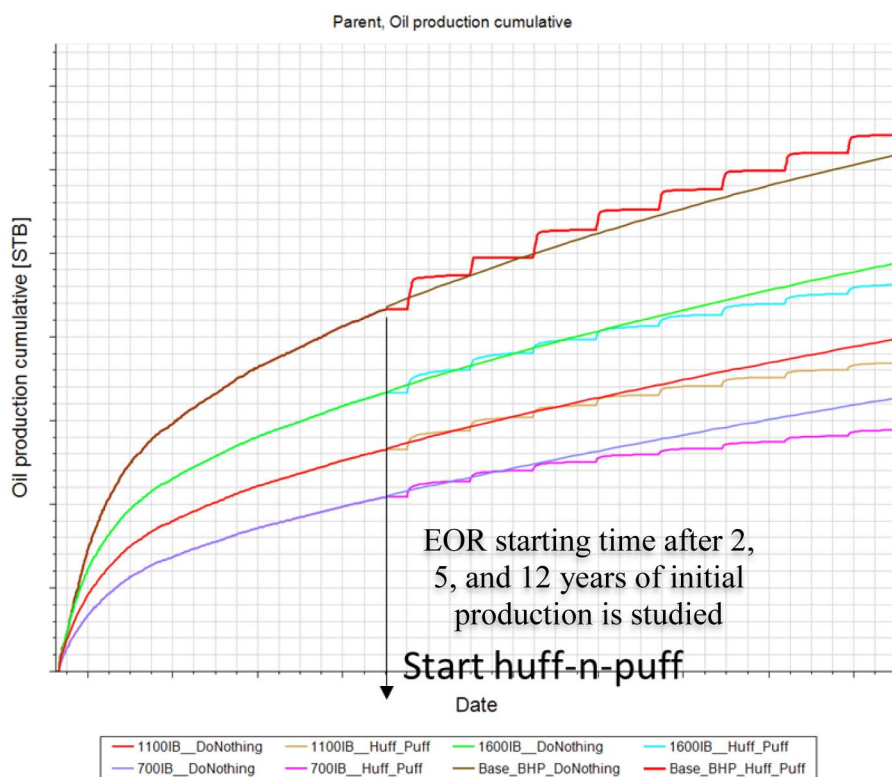


Figure 10—Incremental production gain with huff-n-puff for different treatment size.

Table 3—Incremental production at 1,800-lbm/ft treatment design yielded the best results. Poor stimulation efficiency at lower treatment size may have a diminishing effect on EOR effectiveness.

| Beginning of huff-n-puff implementation<br>(Years since first well production) | 2    | 5   | 12 |
|--|------|-----|----|
| Treatment size<br>(lbs/ft)   |      |     |    |
| 1800   | 3%   | 7%  | 9% |
| 1600   | -5%  | -1% | 3% |
| 1100   | -7%  | -4% | 2% |
| 700  | -12% | -6% | 1% |

The impact of beginning time for huff-n-puff injection on the 3-year cumulative was studied as well. The increments of 3%, 7%, and 9% corresponded to the start of huff-n-puff after 2, 5, and 12 years, correspondingly, for the treatment design with 1,800 lbm/ft. The marginal improvement can be attributed to loss of production during the time the well is under injection and soaking in the EOR application method whereas we still produce a considerable amount of oil during the natural depletion.

## Economic Viability

CO<sub>2</sub> EOR has been successfully used in the United States over four decades. The injection of CO<sub>2</sub> into aging oil fields to produce residual oil has helped extend the producing life of some fields by more than 25 years. Access to economical and abundant supplies of CO<sub>2</sub> is the primary driver of successful EOR projects. The volume of CO<sub>2</sub> required per incremental barrel is typically 4.2 Mscf, and, often, approximately 25% of the CO<sub>2</sub> is recycled after the initial phase of injection. Additional costs of operations such as corrosion inhibitors, recycling, and fluid handling, can add another USD 5/bbl. The infrastructure/capital costs were assumed to be USD 1 million per well (Thomas et al. 2016), and the pilot is assumed to be applied on five

wells for EOR. If we assume USD 2.5/Mscf cost for CO<sub>2</sub>, the breakeven point at a USD 50/bbl price of oil would be achieved at 3.3 years with the current EOR design studied in the well with stimulation done at 1,800 lbm/ft if the EOR is started after 12 years of well's natural production. The breakeven may be longer if the EOR is started earlier (Fig. 11).

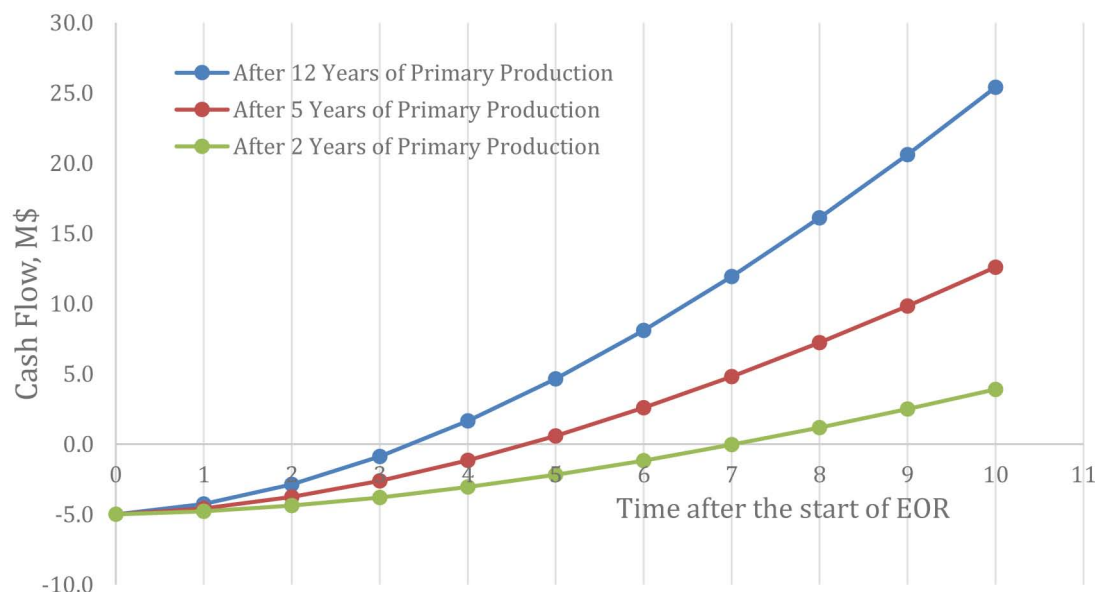


Figure 11—Cash flow curve with EOR methods applied on the 1,800-lbm/ft well completions design for the hydraulic fracture.

Optimizing and improving EOR performance would be crucial to make the process more economic and profitable. Reducing operating cost and planning more wells per section can improve the return on investment. Effective hydraulic fracture stimulation may be one way to improve the reservoir contact to begin with, and then EOR can be used to boost supplemental productivity.

## Conclusions

- The general workflow for the EOR application (CO<sub>2</sub> huff-n-puff injection) was proposed/evaluated using an Eagle Ford data set. The main evaluation parts included history match of the single-well performance followed by huff-n-puff prediction performance under various sensitivity controls.
- Huff-and-puff can recover more oil compared to the natural depletion scenario. Thus, CO<sub>2</sub> huff-n-puff remains a viable EOR method in the oil region of the Eagle Ford shale. Economic evaluation of the scenarios must be performed to evaluate the optimal strategy of EOR application.
- The huff-n-puff performance was evaluated depending on the treatment size and initial time to start the huff-and-puff scheme. Scenarios with higher treatment design are more favorable because they create greater surface area contact with the reservoir and improve the sweep of the reservoir fluid. The huff-and-puff implementation time after the well's initial production impacts the overall recovery from the wellbore.
- The simulated completion and CO<sub>2</sub> EOR combined scenarios analysis showed that the fracture is a significant factor in controlling CO<sub>2</sub> EOR success in shale oil reservoirs. The fracture intensity has a positive effect on CO<sub>2</sub> EOR. Enhancing the induced fracture network complexity is critical to the well productivity in shale oil reservoirs. It was confirmed that the more surface area created corresponded to a higher cumulative production during the time before huff-n-puff was implemented following the same operation control strategy.

- Cost control and improvement in process economics depends hugely on the operating cost as well as the market prices for hydrocarbons. Declining oil prices may deter the interest of the operators in investing to EOR projects, but proper field management and optimizing the EOR technique application may help adjust the cost to make the huff-n-puff method an economic option in the unconventional reservoirs.

Investigation of production mechanism that can improve performance for huff-n-puff during application in the early time of the well's production was out of the scope of the current paper. We think that the operating parameters for managing the CO<sub>2</sub> EOR huff-n-puff process would need to be tuned according to the induced fracture complexity to reap additional benefits.

## Acknowledgment

We would like to thank Schlumberger for allowing us to publish this work.

## References

- Alfarge, D., Wei, M., Bai, B., and Almansour, A. 2017. Effect of Molecular-Diffusion Mechanism on CO<sub>2</sub> Huff-n-Puff Process in Shale-Oil Reservoirs. Presented at the SPE Kingdom of Saudi Arabia Annual Technical Symposium and Exhibition, Dammam, Saudi Arabia, 24–27 April. SPE-188003-MS. <https://doi.org/10.2118/188003-MS>
- Cipolla, C. L., Fitzpatrick, T., Williams, M. J. et al. 2011a. Seismic-to-Simulation for Unconventional Reservoir Development. Presented at the SPE Reservoir Characterisation and Simulation Conference and Exhibition, Abu Dhabi, UAE, 9–11 October. SPE-146876-MS. <https://doi.org/10.2118/146876-MS>
- Cipolla, C.L., Weng, X., Onda, H., et al. 2011b. New Algorithms and Integrated Workflow for Tight Gas and Shale Completion. Presented at the SPE Annual Technical Conference and Exhibition, Denver, Colorado, USA, 30 October–2 November. SPE-146872-MS. <https://doi.org/10.2118/146872-MS>
- Gakhar, K., Rodionov, Y., Defeu, C. et al. 2017. Engineering an Effective Completion and Stimulation Strategy for In-Fill Wells. Presented at the SPE Hydraulic Fracturing Technology Conference and Exhibition, The Woodlands, Texas, USA, 24–26 January. SPE-184835-MS. <https://doi.org/10.2118/184835-MS>
- Gamadi, T. D., Sheng, J. J., Soliman, M. Y. et al. 2014. An Experimental Study of Cyclic CO<sub>2</sub> Injection to Improve Shale Oil Recovery. Presented at the SPE Improved Oil Recovery Symposium, Tulsa, Oklahoma, USA, 12–16 April. SPE-169142-MS. <https://doi.org/10.2118/169142-MS>
- Hoffman, B. T. 2018. Huff-N-Puff Gas Injection Pilot Projects in the Eagle Ford. Presented at the SPE Canada Unconventional Resources Conference, Alberta, Canada, 13–14 March. SPE-189816-MS. <https://doi.org/10.2118/189816-MS>
- Orangi, A., Nagarajan, N. R., Honarpour, M. M. et al. 2011. Unconventional Shale Oil and Gas-Condensate Reservoir Production, Impact of Rock, Fluid, and Hydraulic Fractures. Presented at the SPE Hydraulic Fracturing Technology Conference, The Woodlands, Texas, USA, 24–26 January, SPE-140536-MS. <https://doi.org/10.2118/140536-MS>
- Thomas, W. R., Helms, L. W., Driggers T. K. et al. 2016. EOG Resources (EOG) Earnings Call. 6 May.
- Tovar, F. D., Eide, O., Graue, A. et al. 2014. Experimental Investigation of Enhanced Recovery in Unconventional Liquid Reservoirs using CO<sub>2</sub>: A Look Ahead to the Future of Unconventional EOR. Presented at the SPE Unconventional Resources Conference, The Woodlands, Texas, 1–3 April. SPE-169022-MS. <https://doi.org/10.2118/169022-MS>
- Weng, X., Kresse, O., Cohen, C. et al. 2011. Modeling of Hydraulic Fracture Network Propagation in a Naturally Fractured Formation. Presented at the SPE Hydraulic Fracturing Technology Conference and Exhibition, The Woodlands, Texas, USA, 24–26 January. SPE-140253-MS. <https://doi.org/10.2118/140253-MS>